Title: Skeletal muscle mitochondrial and lipid droplet content assessed with standardized grid sizes for stereology.
Authors: Broskey N.T., Daraspe J., Humbel B.M., Amati F.
Journal: Journal of Applied Physiology
Year: 2013 Sep 1
DOI: 10.1152/japplphysiol.00063.2013

Title: Skeletal muscle mitochondrial and lipid droplet content assessed with standardized grid sizes for stereology

Authors:
Nicholas T. Broskey[1]
Jean Daraspe[2]
Gerald Gremion[3]
Didier Hans[4]
Leopold Schlueter[5]
Bruno M. Humbel[2]
Francesca Amati[1]

Author contributions:
N.T. Broskey: collected data, wrote manuscript
J. Daraspe: collected data
G. Gremion: supervised exercise testing in sports medicine
D. Hans: supervised and checked data quality in radiology
L. Schlueter: supervised stress tests in cardiology
B.M. Humbel: supervised and created electron microscopy protocol
F. Amati: principal investigator, performed biopsies, wrote manuscript

Affiliation:
[1] Department of Physiology, University of Lausanne, Lausanne, Switzerland
[2] Electron microscopy facility, University of Lausanne, Lausanne, Switzerland
[3] Sports Medicine Unit, University Hospital, Lausanne, Switzerland
[4] Center for Bone Disease, Bone & Joint Department, University Hospital, Lausanne, Switzerland
[5] Service of Cardiology, University Hospital, Lausanne, Switzerland

Running head: Mitochondria and grid size

Contact information:
Francesca Amati
University of Lausanne, Bugnon 7, Lausanne 1005, Switzerland
Francesca.amati@unil.ch
Phone: + 41-21-692-5552
Fax: + 41-21-692-5505

Keywords: Transmission electron microcopy, point-counting, intramyofibrillar space, volume density, Cavalieri's principle
Word count: Abstract 250. Text not including abstract, tables and figures: 2749

Number of tables and figures: 4 figures and 3 tables

Abstract

Skeletal muscle mitochondrial (Mito) and lipid droplet (Lipid) content are often measured in human translational studies. Stereological point counting allows computing Mito and Lipid volume density (Vd) from micrographs (M) taken with transmission electron microscopes (TEM). Former studies are not specific as to the size of individual squares that make up the grids, making reproducibility difficult, particularly when different magnifications are used. Our first objective was to determine which size grid would be best at predicting fractional volume efficiently without sacrificing reliability and to test a novel method to reduce sampling bias. The second aim was to assess MitoVd with the standardized grid before and after an exercise intervention. **Methods:** Ten subjects underwent *vastus lateralis* biopsies. Samples were fixed, embedded and cut longitudinally in ultrathin sections of 60 nm. 20 M from the intramyofibrillar region were taken per subject at 33'000x. Different grid sizes were superposed on each M: 1000x1000nm, 500x500nm and 250x250nm. After determination of the most appropriate grid, we assessed the effects of 4 months of endurance training on MitoVd of 10 sedentary adults. **Results:** Mean Mito and Lipid Vd were not statistically different across grids. Variability was greater when going from 1000x1000nm to 500x500nm grid than from 500x500nm to 250x250nm grid. **Discussion:** This study is the first to attempt to standardize grid size while keeping with the conventional stereology principles. This is all in hopes of producing replicable assessments that can be obtained universally across different studies looking at human skeletal muscle mitochondrial and lipid droplet content.

Introduction

Clinical and translational research use electron microscopy methods to assess content of subcellular organelles of interest. Human skeletal muscle mitochondrial volume density is often used as a marker of mitochondrial content. This is particularly true in exercise science research (6, 17), in obesity (4, 9, 18) and diabetes (12, 14, 15).

Mitochondrial volume density is defined as the volume of skeletal muscle occupied by the mitochondria and is measured by the stereological point counting method (22). This is computed by applying a grid with intersecting lines on a two-dimensional image and counting the numbers of points, defined as an intersection on the grid. The percentage of muscle covered by mitochondria is derived from the number of times the mitochondria touches a point divided by the total number of points over the whole image.

Although this is a common technique to measure mitochondria (or lipid droplets) volume density in human skeletal muscle, former literature is not specific as to the size of grids or even further, the size of individual squares that make up the grids (5, 17, 19, 20). This makes reproducibility across existing studies difficult, particularly when different magnifications are used across different microscopes and tissue orientation. Our objective was to determine which size grid would be the best in predicting mitochondrial volume density the most efficiently in the least amount of time without sacrificing reliability, while at the same time being precise in the description of grid size to allow reproducibility across studies located at multiple sites and/or using multiple microscopes. In this study, three grids of varying size squares and total points were utilized for the point counting technique to elucidate and attempt to standardize grid sizes for mitochondrial volume density. It is hypothesized that the grid with the smallest squares and therefore most points would be the most accurate and reliable grid.

In addition to mitochondrial volume density, a secondary aim of this paper is to analyze reliability and efficiency of grid sizes for the measure of intramyocellular lipid droplets volume density.

Furthermore, sampling bias is an important limitation in microscopy. Indeed, sampling should be random which is almost impossible to do when there is a human eye looking through the objectives and selecting which field will be used for photography. Thus another goal of this study was to attempt a semi-blinded method to acquire images to limit biased sampling.

Finally, after achieving the objectives described above, we tested the standardized grid to evaluate mitochondrial volume density response in sedentary older subjects before and after an exercise intervention.

Methodology

Ten volunteers were included in the first part of this study. After signing the IRB consent, subjects underwent a *vastus lateralis* muscle biopsy in fasted and standardized conditions as described elsewhere (1). Muscle strips of about 4 mm^3 were used for electron microscopy. The fixation technique was chosen to enhance membrane contrast and define mitochondria boundaries, thus we fixed in glutaraldehyde solution (EMS, Hatfield, PA, US) 2.5% in Phosphate Buffer Saline (PBS 0.15M pH7.4) (Sigma, St Louis, MO, US) during 30 minutes at room temperature (RT) directly in the operating room. We then replaced the fixative by a fresh mixture of glutaraldehyde 2.5% in osmium tetroxide 1% (EMS, Hatfield, PA, US) with 1.5% of potassium ferrocyanide (Sigma, St Louis, MO, US) in PBS buffer during 1h30 at RT. The samples were then washed two times in distilled water and dehydrated in acetone solution (Sigma, St Louis, MO, US) at graded concentrations (30%-20min; 70%-20min; 100%-1h; 100%-2h). This was followed by infiltration in Epoxy resin (43.5% Epoxy medium, 36.5% DDSA, 18.5% MNA, 1.5% DMP30) (Sigma, St Louis, MO, US) at graded concentrations (Epoxy 1/3 acetone-

2h; Epoxy 3/1 acetone-2h, Epoxy 1/1-4h; Epoxy 1/1-12h) and finally polymerized for 48h at 60°C in an oven. Ultrathin sections of 60nm were cut longitudinally to the muscle fibers on a Leica Ultracut (Leica Mikrosysteme GmbH, Vienna, Austria) and picked up on a nickel slot grid 2x1mm (EMS, Hatfield, PA, US) coated with a polystyrene film (Sigma, St Louis, MO, US). Sections were poststained with uranyl acetate (Sigma, St Louis, MO, US) 4% in H_2O during 10 minutes, rinsed several times with H_2O followed by Coggeshall (21) lead citrate 0.4% in H_2O (Sigma, St Louis, MO, US) during 10 minutes and rinsed several times with H_2O.

Twenty micrographs of the intramyofibrillar region were taken per subject with a transmission electron microscope Philips CM100 (FEI, Eindhoven, The Netherlands) at an acceleration voltage of 80kV and 33,000x of magnification with a pixel size of 2.11nm and a horizontal field width of 8.3µm, with a Megaview III SIS digital camera (Olympus Soft Imaging Solutions GmbH, Münster, Germany) using the software SIS iTEM Megaview III (Olympus Soft Imaging Solutions GmbH, Münster, Germany). To avoid sampling bias, all images were taken using the Multiple Image Alignment plugin (MIA) of the iTEM software. The MIA plugin is a panorama-image function that allows acquisition of a larger image of the sample than the one observed, by an automatic displacement of the sample under the electron beam. The micrographs are composed of an alignment of 4 images in the X-axis per 5 images in the Y-axis, creating a large single micrograph of 20 images without changing the magnification as presented in Figure 1.

Three different sizes of grids were superposed on each micrograph and compared with squares of 1000x1000nm sides (corresponding to $1\mu m^2$), 500x500nm ($0.25\mu m^2$) and 250x250nm ($0.0625\mu m^2$). Upon placing each grid on the same image, the number of points (defined as two intersecting grid lines) that touched mitochondria (or lipid droplets) were tallied and divided by the total number of points on the grid. The total points corresponded to 56 for the 1000x1000nm grid (Figure 2 panel A), 240 for the 500x500nm grid (Figure 2 panel B), and 1023 for the 250x250nm grid (Figure 2 panel C). This process

was repeated for the other 19 images and averaged together to receive the volume density percentage for each grid.

Comparisons between grid sizes were performed with a one way within subjects ANOVA. Variability was assessed with coefficients of variation and Spearman correlations. Intra-rater reliability was evaluated with a second reading of 120 micrographs (all images of six subjects) performed by the first author three months after the first reading in a blinded manner. Inter-rater reliability was also performed in a blinded fashion by the senior author who read 20 micrographs randomly selected. Both intra- and inter-rater reliability were explored with coefficients of variation.

For the second part of the study, 10 volunteers were recruited for four months of exercise training with a pre/post-intervention design. All volunteers were sedentary (≤1 structured exercise session/week) and between 60 and 80 years of age. They were excluded if they had any chronic disease that could either impair mitochondrial biogenesis (e.g. diabetes) or put them at risk for exercising (e.g. uncontrolled hypertension or recent cardiovascular events). After signing IRB consent, subjects underwent a baseline evaluation that encompassed: anthropometric measures (weight and height), dual-energy X-ray absorptiometry (DXA) (Discovery, Hologic Inc., Bedford, MA), peak aerobic capacity (VO_2peak) and *vastus lateralis* biopsy. The same procedures were performed at the end of 16 weeks of exercise. VO_2peak was measured as described previously (2) using a graded exercise protocol on an electronically braked cycle ergometer (Lode B.V., Groningen, The Netherlands) to determine changes in physical fitness and to decide exercise prescription based on their maximal HR. HR, blood pressure and ECG were recorded at each step. VO2 was computed via indirect calorimetry (Metalyzer 3B, Cortex GmbH, Leipzig, Germany). Percutaneous muscle biopsy samples were obtained in the fasted state and processed as described above for the first part of this study.

The 16 week exercise intervention consisted of moderate-intensity supervised endurance training as described previously (3). Subjects were asked to engage in three supervised exercise

sessions per week. Each session was progressively increased to a total of 30 to 60 minutes. Subjects could bike, walk or run with an intensity of 75% of their peak HR. HR monitors (Polar Electro Oy, Kempele, Finland) were used to assess exercise intensity at all times. Exercise prescription was adapted after 8 weeks from a submaximal exercise test.

Results

Ten subjects (6 men and 4 women) were included in the first part of this study. Mean age was 63.0 ± 13.2 years (range 27–76), mean weight 72.6 ± 12.5 kg (range 60.0–102.3), and mean BMI 24.7 ± 3.7 kg/m2 (range 21.0–31.9).

Mitochondrial volume density (MitoVd) computed from the different grids are presented in Table 1 panel A. No significant differences were found with the repeated measures ANOVA. Taking into account the sum of the total points across the 20 micrographs for each subject (Figure 3 panel A), the variability was greater when going from the 1000x1000nm to the 500x500nm grid than when going from the 500x500nm to the 250x250nm grid. Indeed, the coefficient of variation (CV) was of 7.00 ± 1.41% between grids 1000x1000nm and 500x500nm, while the CV was 4.75 ± 1.44% between grids 500x500nm and 250x250nm. Spearman Rho's correlations were of 0.90 between 1000x1000nm and 500x500nm grid and 0.99 between 500x500nm and 250x250nm grid ($P=0.003$ and $P<0.0001$ respectively).

Lipid droplet volume density (LipidVd) computed from the different grids are presented in Table 1 panel B and Figure 3 panel B. Following the same pattern as for mitochondria volume density, the variability was greater when going from the 1000x1000nm to the 500x500nm grid than when going from the 500x500nm to the 250x250nm grid. CVs were 15.02 ± 4.74% between grids 1000x1000nm and 500x500nm, and 5.22 ± 1.22% between grids 500x500nm and 250x250nm. Spearman Rho's

correlations were of 0.83 between grids 1000x1000nm and 500x500nm and 0.93 between grids 500x500nm and 250x250nm (P=0.003 and P<0.0001 respectively).

Due to these results, plus the practicality that it takes less time to analyse the 500x500nm than the 250x250nm, we chose the 500x500nm standardized grid for the second part of this study and to assess intra- and inter-rater reliability. As described above, a second reading of 120 micrographs (20 micrographs of 6 subjects) was performed 3 months after the first reading, mean CV was 6.38 ± 0.70 % for MitoVd and 3.54 ± 0.91% for LipidVd. Between the first and second reading for MitoVd Spearman rho was 0.963 (P<0.0001) and for LipidVd rho was 0.942 (P<0.0001). Inter-rater reliability was assessed on 20 micrographs and resulted in a CV of 6.57 ± 1.17 % for MitoVd and 11.93 ± 3.39% for LipidVd. Spearman correlations were 0.95 (P<0.0001) for MitoVd and 0.97 (P<0.0001) for LipidVd.

The characteristics of the 10 subjects that took part in the pre/post-exercise intervention are presented in table 2. The effects of endurance exercise were significant with an average increase of 60.43 ± 17.27% in MitoVd, 48.98 ± 19.60% in LipidVd and 15.89 ± 4.70% for VO_2peak (table 2). Figure 4 presents the individual changes in MitoVd and LipidVd. Although subjects were asked not to change their habitual diets, they lost on average 1.52 ± 0.83 % of their weight and 5.92 ± 1.90% of body adiposity (table 2).

Discussion

The evaluation of the fractional volume of muscle cells occupied by mitochondria and lipid droplets may be performed by the common stereological methodology to reduce it to their fractional area in random sections. This methodology has been reconducted to Delesse in 1946 (22) and back to Cavalieri in 1635 (8) and is widely used in quantitative stereological assessment. The objective of this study was to define a specific grid size to allow reliability and reproducibility across studies and electron microscopes of different study sites. The lattice distance of the superimposed grid or,

equivalently, the number of longitudinal and vertical lines defining the grid that covers the microscope slice photograph, depend of course on the average fractional area to be determined. Knowing that the order of magnitude occupied by mitochondria is around 2 to 5 percent (1), we have investigated three grid sizes (1000x1000nm, 500x500nm and 250x250nm) with a respective total of intersections points of around 56, 240 and 1023, in order to determine the stability of the corresponding fraction of points falling into our examined structures.

From figure 3, we see that the factional area varies greatly going from 1000x1000nm to 500x500nm, while changes slightly going from 500x500nm to 250x250nm. This is confirmed by the statistical results and coefficients of variations. Due to the stability of the results between the 500x500nm and the 250x250 nm grid, while the later is more time-consuming, we have assessed the inter- and intra-reliability of the method with the 500x500nm grid. The results are adequate and allow an accurate measure of fractional volume of the muscle cells occupied by mitochondria and lipid droplets.

Although multiple groups have published with this technique for the evaluation of myocytes' subcellular organelles, we were unable to find precise and reliable data in regards to lattice size of grids (6, 11, 17, 18, 20). As each electron microscope is unique and different researchers use different magnifications, describing the number of points used but not the size of the grids makes comparison across sites and studies difficult. In order to compare results from different groups using different magnifications, we believe that the utilization of standardized grids is of interest to allow reproducibility and comparison across research centers.

We noticed that the number of total points falling into mitochondria with the 500x500nm grid is on average 240 points per micrograph while it is around 1023 with the 250x250nm grid and 56 with the 1000x1000nm grid. These results agree reasonably with the Cavalieri's principle that states that a total of around 100-200 test points in a compartment provide a quite correct estimation of fractional

volume of that compartment (16) and that counting beyond 200 points does not add significant precision.

Using the 500x500nm grid to assess changes in MitoVd in our cohort of older sedentary volunteers indicated baseline intramyofibrillar MitoVd on average of 4.7% and 7.3% after four months of endurance training. This magnitude of change in mitochondrial content with exercise is similar to the one observed by Menshikova et al. (13). In a 12 week endurance exercise (4 moderate intensity sessions/week) intervention with 8 older sedentary volunteers (mean 67 years old), they observed a 56% improvement in mitochondrial content using mitochondrial DNA measures. Early stereological assessment in muscle by Hoppeler et al. (10) performed with stereological measures presented a 33% change in MitoVd with 6 weeks of training (5 high intensity cycling/week) in 10 young adults (mean 29 years old). They used a lower magnification (24'000x) and applied a non-standardized grid with 100 points. At baseline, their volunteers had an average relative VO_2peak of 43.2 ± 6.3 ml/min/kg of body weight and a MitoVd of 3.76 ± 0.22%. At the end of the 6 weeks of training, VO_2peak improved by 13.8% reaching 49.3 ± 5.7 ml/min/kg and MitoVd improved by 31.6% reaching 5.0 ± 0.2%. In the present study, although VO2peak values are lower as expected in 10 older sedentary volunteers (25.1 ± 2.6 at baseline and 29.0 ± 2.6 ml/min/kg of body weight after training), MitoVd are higher at both time points. Although some discrepancies may be explained by the different training protocols or subjects' characteristics, the lack of standardization in the stereology assessment explains in part these differences, thus the need for a standardized grid that can be used across microscopes and different magnifications.

Using the 500x500nm grid to assess changes in LipidVd in our cohort of older sedentary volunteers indicated baseline intramyofibrillar lipid droplet content on average of 1.35% and 1.86% after four months of endurance training. This magnitude of change is similar to our previous study (7), where we found a 41% increase in intramyocellular lipids measured by histochemistry (Oil Red O

staining) in a comparable population and intervention. Tarnopolsky et al. (17) also observed this magnitude in response (42%) in younger volunteers after 7 weeks of endurance exercise measured by circling of the lipid droplets on TEM micrographs at a magnitude of 6'500x. Thus we are confident that the proposed method is reliable to report intervention effects also for intramyocellular lipids.

This study is the first to attempt to standardize grid size while keeping with the conventional principles implemented in the past by Cavalieri. In doing so, it is now possible for studies to revisit not only the number of total points on the grid, but also make attention to individual sizes of each square on the grid. The advantage is that researchers can calibrate the grid on size (in nanometers), thus keeping always the same measure across different microscopes. This is all in hopes of producing replicable stereological assessments that can be obtained universally across various domains of science, whether that is for diabetes, obesity, or exercise purposes.

Acknowledgments:

We appreciate the cooperation of our research volunteers and the nursing staff, Christiane Pellet and Francoise Secretan, from the Clinical Research Center of the University Hospital of the University of Lausanne (CHUV). Ours thanks to Chantal Daucourt for her assistance in the exercise lab, the DXA technicians and to Jean-Pierre Sacco, who allowed us to use the *Fit Point* gym for the supervised training. We are grateful to Daniele Amati who provided his physics expertise.

Parts of this work has been accepted and presented at the annual scientific meeting of the American College of Sports Medicine in May 2012.

Grants:

This study was supported by the Swiss National Science Foundation Ambizione grant FNS PZ00P3_126339 (to F.A.) and BASPO grant (to F.A.). The Electron Microscopy Facility is supported by the School of Biology and Medicine at the University of Lausanne.

Disclosures:

No conflicts of interest to disclose.

Author contributions:

Nicholas T. Broskey performed experiments, analyzed data, prepared figures and drafted manuscript. Jean Daraspe performed experiments and analyzed data. Gerald Gremion supervised exercise testing in sports medicine. Didier Hans supervised and checked data quality for DXA scans. Leopold Schlueter supervised stress tests EKGs and gave cardiology expertise. Bruno M. Humbel supervised electron microscopy work, edited and revised manuscript. Francesca Amati instigated the project, interpreted results and wrote the manuscript.

References:

1. **Amati F, Dube JJ, Alvarez-Carnero E, Edreira MM, Chomentowski P, Coen PM, Switzer GE, Bickel PE, Stefanovic-Racic M, Toledo FG, and Goodpaster BH**. Skeletal muscle triglycerides, diacylglycerols, and ceramides in insulin resistance: another paradox in endurance-trained athletes? *Diabetes* 60: 2588-2597, 2011.

2. **Amati F, Dube JJ, Shay C, and Goodpaster BH**. Separate and combined effects of exercise training and weight loss on exercise efficiency and substrate oxidation. *Journal of applied physiology* 105: 825-831, 2008.

3. **Amati F, Dube JJ, Stefanovic-Racic M, Toledo FG, and Goodpaster BH**. Improvements in insulin sensitivity are blunted by subclinical hypothyroidism. *Medicine and science in sports and exercise* 41: 265-269, 2009.

4. **Boyle KE, Zheng D, Anderson EJ, Neufer PD, and Houmard JA**. Mitochondrial lipid oxidation is impaired in cultured myotubes from obese humans. *International journal of obesity* 2011.

5. **Chomentowski P, Coen PM, Radikova Z, Goodpaster BH, and Toledo FG**. Skeletal muscle mitochondria in insulin resistance: differences in intermyofibrillar versus subsarcolemmal subpopulations and relationship to metabolic flexibility. *The Journal of clinical endocrinology and metabolism* 96: 494-503, 2011.

6. **Devries MC, Lowther SA, Glover AW, Hamadeh MJ, and Tarnopolsky MA**. IMCL area density, but not IMCL utilization, is higher in women during moderate-intensity endurance exercise, compared with men. *American journal of physiology Regulatory, integrative and comparative physiology* 293: R2336-2342, 2007.

7. **Dube JJ, Amati F, Toledo FG, Stefanovic-Racic M, Rossi A, Coen P, and Goodpaster BH**. Effects of weight loss and exercise on insulin resistance, and intramyocellular triacylglycerol, diacylglycerol and ceramide. *Diabetologia* 54: 1147-1156, 2011.

8. **Gundersen HJ, Bendtsen TF, Korbo L, Marcussen N, Moller A, Nielsen K, Nyengaard JR, Pakkenberg B, Sorensen FB, Vesterby A, and et al.** Some new, simple and efficient stereological methods and their use in pathological research and diagnosis. *APMIS : acta pathologica, microbiologica, et immunologica Scandinavica* 96: 379-394, 1988.

9. **Holloway GP, Bonen A, and Spriet LL**. Regulation of skeletal muscle mitochondrial fatty acid metabolism in lean and obese individuals. *The American journal of clinical nutrition* 89: 455S-462S, 2009.

10. **Hoppeler H, Howald H, Conley K, Lindstedt SL, Claassen H, Vock P, and Weibel ER**. Endurance training in humans: aerobic capacity and structure of skeletal muscle. *Journal of applied physiology* 59: 320-327, 1985.

11. **Hoppeler H, Mathieu O, Krauer R, Claassen H, Armstrong RB, and Weibel ER**. Design of the mammalian respiratory system. VI Distribution of mitochondria and capillaries in various muscles. *Respiration physiology* 44: 87-111, 1981.

12. **Kelley DE, He J, Menshikova EV, and Ritov VB**. Dysfunction of mitochondria in human skeletal muscle in type 2 diabetes. *Diabetes* 51: 2944-2950, 2002.

13. **Menshikova EV, Ritov VB, Fairfull L, Ferrell RE, Kelley DE, and Goodpaster BH**. Effects of exercise on mitochondrial content and function in aging human skeletal muscle. *The journals of gerontology Series A, Biological sciences and medical sciences* 61: 534-540, 2006.

14. **Mogensen M, Sahlin K, Fernstrom M, Glintborg D, Vind BF, Beck-Nielsen H, and Hojlund K**. Mitochondrial respiration is decreased in skeletal muscle of patients with type 2 diabetes. *Diabetes* 56: 1592-1599, 2007.

15. **Phielix E, Meex R, Moonen-Kornips E, Hesselink MK, and Schrauwen P**. Exercise training increases mitochondrial content and ex vivo mitochondrial function similarly in patients with type 2 diabetes and in control individuals. *Diabetologia* 53: 1714-1721, 2010.

16. **Roberts N, Cruz-Orive LM, Reid NM, Brodie DA, Bourne M, and Edwards RH**. Unbiased estimation of human body composition by the Cavalieri method using magnetic resonance imaging. *Journal of microscopy* 171: 239-253, 1993.

17. **Tarnopolsky MA, Rennie CD, Robertshaw HA, Fedak-Tarnopolsky SN, Devries MC, and Hamadeh MJ**. Influence of endurance exercise training and sex on intramyocellular lipid and mitochondrial ultrastructure, substrate use, and mitochondrial enzyme activity. *Am J Physiol-Reg I* 292: R1271-R1278, 2007.

18. **Toledo FG, Menshikova EV, Azuma K, Radikova Z, Kelley CA, Ritov VB, and Kelley DE**. Mitochondrial capacity in skeletal muscle is not stimulated by weight loss despite increases in insulin action and decreases in intramyocellular lipid content. *Diabetes* 57: 987-994, 2008.

19. **Toledo FG, Menshikova EV, Ritov VB, Azuma K, Radikova Z, DeLany J, and Kelley DE**. Effects of physical activity and weight loss on skeletal muscle mitochondria and relationship with glucose control in type 2 diabetes. *Diabetes* 56: 2142-2147, 2007.

20. **Toledo FG, Watkins S, and Kelley DE**. Changes induced by physical activity and weight loss in the morphology of intermyofibrillar mitochondria in obese men and women. *The Journal of clinical endocrinology and metabolism* 91: 3224-3227, 2006.

21. **Venable JH, and Coggeshall R**. A Simplified Lead Citrate Stain for Use in Electron Microscopy. *The Journal of cell biology* 25: 407-408, 1965.

22. **Weibel ER, Kistler GS, and Scherle WF**. Practical stereological methods for morphometric cytology. *The Journal of cell biology* 30: 23-38, 1966.

Figure captions

Figure 1 Example of acquisition with the Multiple Image Alignment plugin. Panel A displays the field of view as observed in the objective of the electron microscope at 33'000x. This image corresponds to a surface of 2.982µm x 2.236µm and 1376 x 1032 pixels. Panel B shows the larger area around the previous view (square) after alignment and overlap of 20 single images captured blindly by the electron microscope (36% in horizontal and 34% in vertical). The new image measures are 8.259µm x 7.89µm and 3914 x 3739 pixels. The bottom white line is 2µm.

Figure 2 Example of point counting with three different grid sizes on one micrograph. Panel A, grid 1000x1000 nm. Panel B, grid 500x500 nm. Panel C, grid 250x250 nm. One intersection = one point, mitochondria points = white star, lipid droplets points = black star.

Figure 3 Mitochondria and lipid droplet volume density as a function of total points counted for each sample. Panel A, mitochondrial volume density. Panel B, lipid droplet density. X-axis represents the average of total points (intersections) across 20 micrographs analyzed for each subject. Each line represents a different subject.

Figure 4 Mitochondria and Lipid droplet: individual responses with endurance exercise. Panel A, Mitochondrial volume density. Panel B, Lipid droplet volume density. Each line represents a different subject, circles are group average (Paired T test, $P<0.01$).

Table 1: Mitochondria and lipid droplet volume density computed with different size grids

A	**Mean ± SE**	**Minimum**	**Maximum**
MitoVD (%) with 1000x1000nm grid	6.395 ± 0.714	3.479	10.056
MitoVD (%) with 500x500nm grid	6.077 ± 0.701	3.097	10.021
MitoVD (%) with 250x250nm grid	6.368 ± 0.797	3.189	11.628
B	**Mean ± SE**	**Minimum**	**Maximum**
LipidVD (%) with 1000x1000nm grid	1.275 ± 0.253	0.446	3.125
LipidVD (%) with 500x500nm grid	1.414 ± 0.234	0.771	2.854
LipidVD (%) with 250x250nm grid	1.379 ± 0.206	0.702	2.553

Table 2: Exercise intervention - Subject characteristics

	Pre	Post	Paired T-test (one sided-P value)
age (years)	65.9±2.60 (63-71)		
gender	6 men/4 women		
weight (kg)	86.6±17.6 (62.2-106.6)	85.1±16.6 (59.9-102.6)	**0.040**
BMI (kg/m^2)	28.3±4.5 (21.4-33.8)	27.8±4.2 (21.1-32.9)	**0.034**
fat free mass (kg)	59.0±12.4 (42.3-74.0)	59.6±11.9 (44.1-74.9)	0.069
fat mass (kg)	28.9±10.7 (11.8-45.9)	27.0±10.3 (9.1-43.1)	**0.002**
body fat (%)	32.4±9.6 (18.5-45.6)	30.7±9.6 (14.9-43.7)	**0.001**
VO_2peak (ml/min)	2101±522 (1328-2804)	2395±522 (1790-3318)	**0.008**
VO_2peak/FFM (ml/min/kg)	35.80±6.88 (28.78-48.06)	40.60±6.99 (31.63-50.22)	**0.004**
MitoVd (%)	4.723±1.222 (3.097-6.360)	7.301±1.944 (3.396-9.271)	**0.0009**
LipidVd (%)	1.346±0.698 (0.396-2.464)	1.855±1.043 (0.683-4.402)	**0.014**

Caption: Results are mean±SD (min-max), VO_2peak=peak oxygen consumption, MitoVd=Mitochondria volume density, LipidVd=Lipid droplet volume density.

Figure 1
A

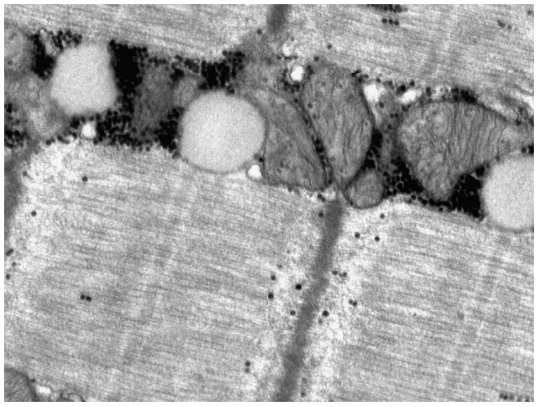

B

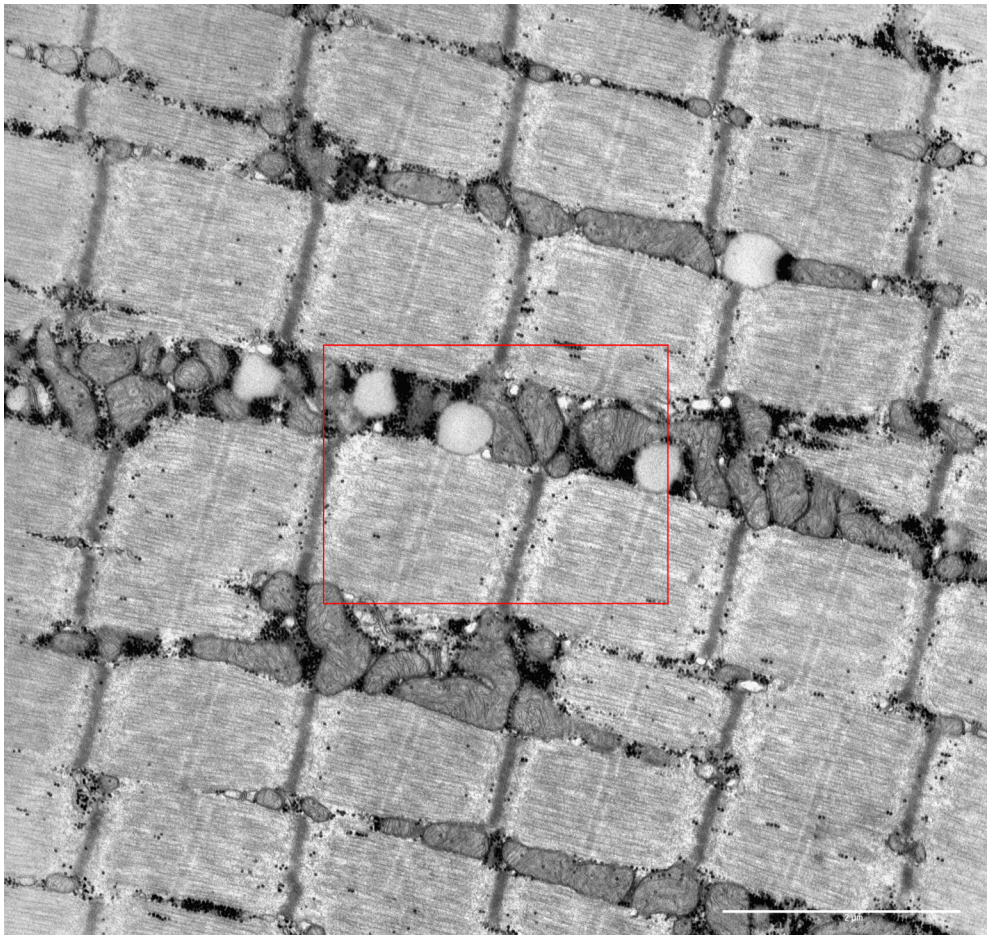

Figure 2

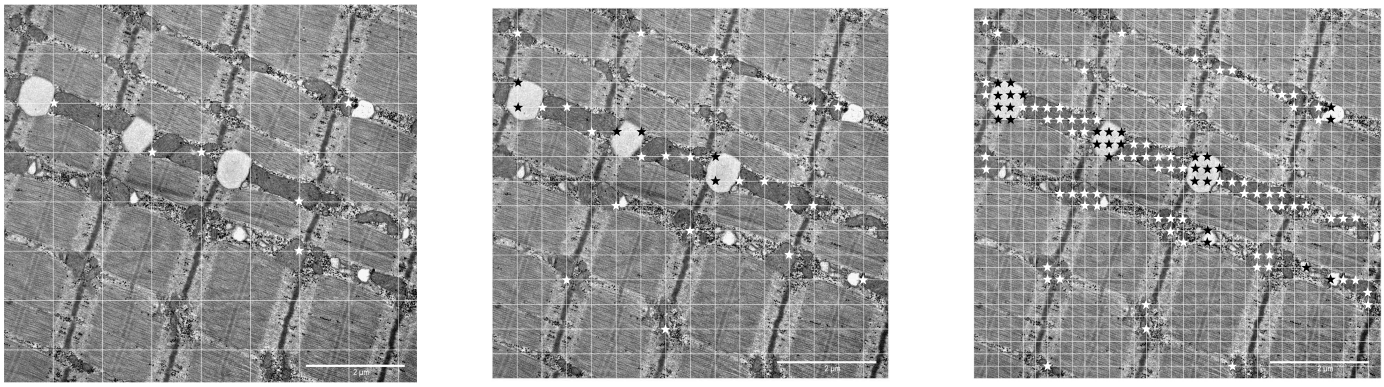

Figure 3

Figure 3, panel A

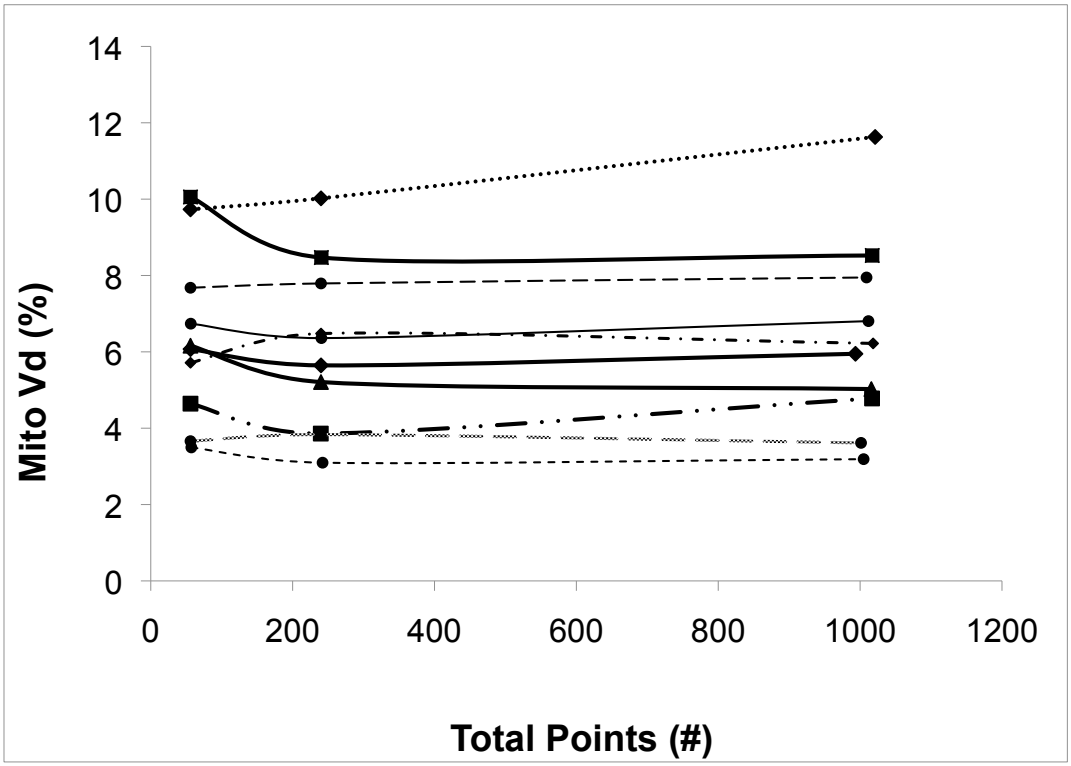

Figure 4

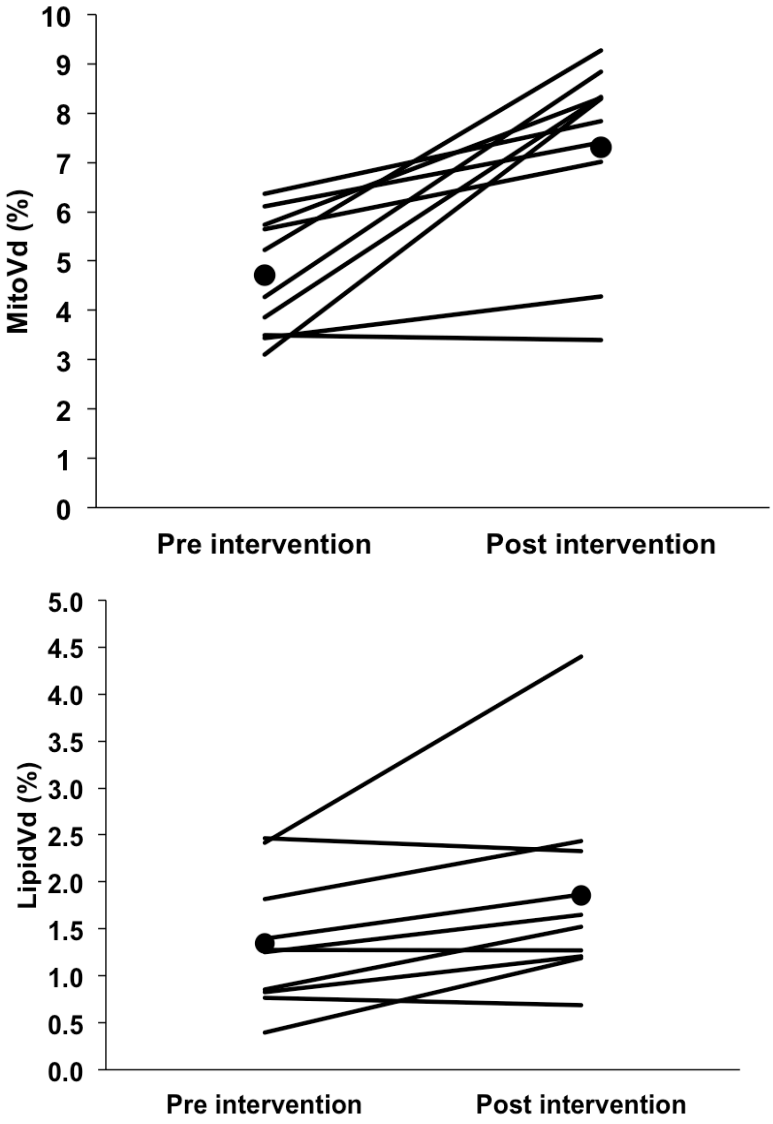
10
9
8
7
6
5
4
3
2
1
0
MitoVd (%)
Pre intervention
Post intervention
5.0
4.5
4.0
3.5
3.0
2.5
2.0
1.5
1.0
0.5
0.0
LipidVd (%)
Pre intervention
Post intervention